HHS Public Access

Author manuscript

Eur J Nucl Med Mol Imaging. Author manuscript; available in PMC 2019 July 01.

Published in final edited form as:

Eur J Nucl Med Mol Imaging. 2018 July ; 45(8): 1372–1381. doi:10.1007/s00259-018-3941-3.

ImmunoPET imaging of CD38 in murine lymphoma models using ^{89}Zr-labeled daratumumab

Lei Kang[1,3,#], **Dawei Jiang**[2,3,#], **Christopher G. England**[4], **Todd E. Barnhart**[4], **Bo Yu**[3], **Zachary T. Rosenkrans**[5], **Rongfu Wang**[1], **Jonathan W. Engle**[4], **Xiaojie Xu**[6,*], **Peng Huang**[2,*], and **Weibo Cai**[3,4,5,7,*]

[1]Department of Nuclear Medicine, Peking University First Hospital, Beijing, 100034, China

[2]Guangdong Key Laboratory for Biomedical Measurements and Ultrasound Imaging, School of Biomedical Engineering, Health Science Center, Shenzhen University, Shenzhen, 518060, China

[3]Department of Radiology, University of Wisconsin - Madison, WI, 53705, USA

[4]Department of Medical Physics, University of Wisconsin - Madison, Madison, WI, 53705, USA

[5]School of Pharmacy, University of Wisconsin - Madison, Madison, WI, 53705, USA

[6]Department of Medical Molecular Biology, Beijing Institute of Biotechnology, Beijing, 100850, China

[7]University of Wisconsin Carbone Cancer Center, Madison, WI, 53705, USA

Abstract

Purpose—CD38 is considered a potential biomarker for multiple myeloma (MM) and has shown a strong link with chronic lymphocytic leukemia due to high and uniform expression on plasma cells. *In vivo* evaluation of CD38 expression may provide useful information about lesion detection and prognosis of treatment in MM. In this study, immunoPET imaging with ^{89}Zr-labeled daratumumab was used for differentiation of CD38 expression in murine lymphoma models to provide a potential noninvasive method for monitoring CD38 in the clinic.

Methods—Daratumumab was radiolabeled with ^{89}Zr ($t_{1/2}$ = 78.4 h) via conjugation with desferrioxamine (Df). After Western blot (WB) was used to screen CD38 expression in five lymphoma cell lines, flow cytometry and cellular binding assays were performed to test the binding ability of labeled or conjugated daratumumab with CD38 *in vitro*. PET imaging and biodistribution studies were performed to evaluate CD38 expression after injection of ^{89}Zr-Df-daratumumab. ^{89}Zr-Df-IgG was also evaluated as a non-specific control group in the Ramos model. Finally, CD38 expression in tumor tissues was verified by histological analysis.

Corresponding Author: Weibo Cai, Room 7137, 1111 Highland Ave, Madison, WI 53705-2275, USA. wcai@uwhealth.org; Phone: 608-262-1749; Fax: 608-265-0614. Peng Huang, Nanhai Ave 3688, Guangdong Key Laboratory for Biomedical Measurements and Ultrasound Imaging, School of Biomedical Engineering, Health Science Center, Shenzhen University, Shenzhen, Guangzhou, 518060, China. peng.huang@szu.edu.cn; Phone: 86-0755-86671911. Xiaojie Xu, Department of Medical Molecular Biology, Beijing Institute of Biotechnology, 27 Tai-Ping Rd, Beijing, 100850, China. miraclexxj@126.com; Phone: 86-010-6693-1830; Fax: 86-010-6824-8045.
[#]These authors contributed equally to this work.

Conflict of Interest: The authors declare that they have no conflict of interest.

Ethical approval: All applicable international, national, and/or institutional guidelines for the care and use of animals were followed.

Results—Using WB screening, the Ramos cell line was found to express the highest level of CD38 while the HBL-1 cell line had the lowest expression. Df-conjugated and ^{89}Zr-labeled daratumumab displayed similar high binding affinities with Ramos cells. PET imaging of ^{89}Zr-Df-daratumumab showed a high tumor uptake of up to 26.6 ± 8.0 %ID/g for Ramos at 120 h post-injection, and only up to 6.6 ± 2.9 %ID/g for HBL-1 (n = 4). Additionally, ^{89}Zr-Df-IgG demonstrated a low tumor uptake in the Ramos model (only 4.3 ± 0.8 %ID/g at 120 h post-injection). *Ex vivo* biodistribution studies showed similar trends with imaging results. Immunofluorescent staining of tumor tissues verified higher CD38 expression of Ramos than that of HBL-1.

Conclusions—The role of ^{89}Zr-Df-daratumumab was investigated for evaluating CD38 expression in lymphoma models noninvasively and was found to be to a promising imaging agent of CD38 positive hematological diseases such as MM in future clinical applications.

Keywords

Daratumumab; Positron emission tomography (PET); CD38; B-cell lymphoma; ImmunoPET; cancer; ^{89}Zr

Introduction

Lymphomas are a highly heterogeneous group of malignancies of the lymphatic system either from B cells or T cells. There are more than 100 types of lymphoma according to the latest version of world health organization (WHO) classification [1]. B-cell derived lymphoma accounts for about 80% of lymphomas. Imaging methods could provide non-invasive and real-time information for lymphoma diagnosis, prognosis and evaluation of therapy in the clinic. ^{18}F-fluorodeoxyglucose (^{18}F-FDG) positron emission tomography (PET) imaging is now widely used for the detection and monitoring of lymphoma [2]. However, this glucose metabolic tracer lacks specificity to detect the differences between malignancies and inflammation [3]. The identification of biomarkers has become a prerequisite factor for treatment decisions. ImmunoPET combines the high sensitivity and resolution of PET imaging with the specificity of monoclonal antibodies (mAbs) [4]. As a result, immunoPET could provide a noninvasive method to assess the target's expression and distribution *in vivo* and would, therefore, be useful for accurate diagnosis, prognosis, and therapeutic evaluation.

CD38 is a 45-kD type II transmembrane glycoprotein that functions in the enzymatic activity of intracellular calcium signaling, receptor-mediated regulation of lymphocyte cell adhesion and signal transduction [5, 6]. CD38 is highly expressed on plasma cells, especially on multiple myeloma (MM) cells. However, CD38 is expressed at relatively low levels on most resting natural killer (NK) cells, monocytes, and other various hematological cell types [7]. This suggests that CD38 is a suitable biomarker for MM [8]. Moreover, CD38 has been found to be an adverse prognostic marker in chronic lymphocytic leukemia [9]. Therefore, evaluation of CD38 expression could provide useful information about the treatment and prognosis of CD38-positive hematologic malignancies.

Daratumumab (Darzalex; Janssen Biotech, Inc) is the first anti-CD38 human immunoglobulin G1 kappa (IgG1-κ) mAb [7, 10]. It was developed from the immunization of human immunoglobulin transgenic mice with recombinant CD38 protein [11]. Daratumumab binds to CD38 and induces the death of CD38-expressing cells via diverse cytotoxic mechanisms that include complement-dependent cytotoxicity, antibody-dependent cytotoxicity, antibody-dependent cellular phagocytosis, apoptosis, and the inhibition of enzymatic activity of CD38 [11–13]. Daratumumab demonstrated therapeutic effects even at low concentrations in a SCID mouse xenograft tumor model [13]. Moreover, daratumumab not only showed inhibitory on MM tumor models but also on B cell tumor models [11], suggesting a potential application in lymphoma.

In our previous study, ^{89}Zr-labeled daratumumab was developed as a PET probe to visualize CD38 expression in lung cancer models [14]. However, the relatively low tumor uptake (highest at 8.1 ± 1.2 %ID/g) limited its potential for lung tumor imaging. To date, there have been no reports about CD38 PET imaging in lymphoma. Herein, we prepare ^{89}Zr-labeled daratumumab for *in vivo* imaging of CD38 expression in different B-cell lymphoma models. We hypothesized that PET imaging using ^{89}Zr-Df-daratumumab would allow for *in vivo* differentiation of CD38 expression and sensitive detection of CD38-positive lymphoma, and therefore for the guidance of clinical treatment.

Materials and methods

Conjugation and radiolabeling

The preparation of ^{89}Zr ($t_{1/2}$ = 78.4 h) radiolabeled daratumumab was performed through conjugation with SCN-Bn-deferoxamine (Df), as described in previous protocols [14, 15]. Briefly, 4 mg of daratumumab was added to 500 μL of PBS and adjusted to a pH of 8.5 – 9.0 with Na_2CO_3 (0.1 M), then Df dissolved in dimethyl sulfoxide was added at a 1:10 molar ratio. The reaction was kept at room temperature (RT) for 2 h. Df-daratumumab was then purified using PD-10 columns (GE Healthcare) with PBS as the mobile phase. For ^{89}Zr labeling, 148 MBq (4 mCi) of ^{89}Zr-oxalate were produced using a PETrace cyclotron (GE Healthcare) and diluted in 0.5 mL of HEPES buffer (0.5 M) at the adjusted pH of 7.0 using Na_2CO_3 (2M). 600 μg (150 μg/mCi) of Df-daratumumab was added and incubated for 1h at 37 °C. The ^{89}Zr-Df-daratumumab product was then purified using PD-10 columns and measured for its radiochemical yields. ^{89}Zr labeled human serum IgG was used as a non-specific control tracer and prepared with similar methods as mentioned above.

Cell culture

Human B lymphocyte cell lines Ramos, Daudi, Raji (Burkitt's lymphoma), Rec-1 (Mantle cell lymphoma), and HBL-1 (Human diffuse large B-cell lymphoma) were purchased from American Type Culture Collection (ATCC, Manassas, VA, USA). Cells were cultured in RPMI 1640 medium supplemented with 10% fetal bovine serum (FBS; Invitrogen) and 1% penicillin/streptomycin (Hyclone) at 37 °C in a humidified incubator with 5% CO_2.

Western blot

For Western blot, lymphoma cells were centrifuged and harvested. Total protein concentration of each cell line was measured using a Pierce Coomassie protein assay kit (ThermoFisher Scientific). 40 μg of total protein was loaded into a 4 – 12% Bolt Bis-Tris Plus gel (ThermoFisher Scientific), along with Chameleon Duo ladder protein marker (LI-COR Biosciences, USA). Electrophoresis was performed at 110 mV and 4 °C for 75 min. All proteins were then transferred to a nitrocellulose membrane using an iBlot 2 (ThermoFisher Scientific) for 7 min. The membrane was blocked with Odyssey blocking buffer (LI-COR, USA) for 1 h at RT and further incubated with a mouse anti-human CD38 antibody (1:1000) and rabbit anti-human β-tubulin antibody (1:2000) overnight at 4 °C. All primary antibodies were purchased from Novus Biologicals (Littleton, CO, USA). Next, the membrane was washed three times with PBS-T (phosphate buffered saline with Tween 20) and incubated with donkey anti-mouse IRDye 800CW and goat anti-rabbit IRDye 680RD secondary antibodies (LI-COR, USA) for 1 h at RT. The washed membrane was scanned and quantitatively analyzed by an Odyssey infrared imaging system (LI-COR, USA).

Flow cytometry

Cells were washed with cold PBS buffer and incubated with Flow Cytometry Staining Buffer Solution (eBioscience, USA) at a concentration of 1×10^6 cells/mL at RT for 1 h. Cells were then incubated with 200 μL of daratumumab (5 or 25 μg/mL in abovementioned buffer) on ice for 60 min and then washed with cold PBS for three times. Cells were incubated with a goat anti-human secondary antibody (3 μg/mL, ThermoFisher Scientific) on ice for 30 min and washed again. The cells were analyzed using a LSRFortessa cell analyzer (BD Biosciences) and mean fluorescence intensities were processed using the FlowJo software (Tree Star, USA).

Receptor binding assay

^{89}Zr-Df-daratumumab was used to determine its cellular binding affinity in Ramos cells. Ramos cells were seeded in a 96-well plate at 1×10^6 cells per well. ^{89}Zr-Df-daratumumab in PBS solution (concentration ranging from 0.03 – 100 nM) was incubated with the cells in each well at RT for 2 h. 1 μmol of unlabeled daratumumab was added to determine the non-specific binding. After 2 h of incubation, cells were washed three times with PBS, then collected and counted with an automated gamma counter (PerkinElmer, USA). The binding results including maximum binding ability (B_{max}), affinity constant (K_a), and receptor density on Ramos cells were determined using GraphPad Prism software (La Jolla, USA).

Animal model

All animal studies were conducted in accordance with protocols approved by the University of Wisconsin Institutional Animal Care and Use Committee. 4 to 6-week-old male CB17-SCID immunodeficient mice, deficient in T and B cells, were bought from Envigo (Indianapolis, IN, USA) and used for implantation of subcutaneous tumors. Each mouse was subcutaneously injected with 1×10^7 lymphoma cells (Ramos or HBL-1) in 200 μL of Matrigel (Invitrogen, USA) into their lower right flank. Mice were monitored every other day for health and tumor volumes.

PET imaging and biodistribution

Tumor-bearing mice (n = 4) were intravenously injected with 5 – 10 MBq of ^{89}Zr-Df-daratumumab. PET scans were conducted at 6, 12, 24, 48, 72, 96, and 120 h after injection on an Inveon micro-PET/CT scanner (Siemens, Germany). 20 million coincidence events were acquired at each time point for each mouse. Tracer accumulation of the heart, liver, spleen, muscle, and tumor was obtained by drawing region-of-interest (ROI) and quantification analysis using the Inveon software. Following 120 h PET scan, mice were euthanized by CO_2 and organs of interest were harvested, including the heart, liver, spleen, lung, kidneys, stomach, intestine, pancreas, tail, skin, muscle, bone, brain, blood, and tumor. All tissue and organs were weighted and their radioactivities were measured using a gamma counter (PerkinElmer, USA). The tracer uptake was denoted by percentage of injected dose per gram of tissue (%ID/g). ^{89}Zr-Df-IgG was also injected in another group of Ramos tumor-bearing mice for PET imaging and biodistribution analysis, to show the non-specific distribution of human monoclonal antibody.

Immunofluorescence staining

Immunofluorescence staining of tumor tissues was performed following standard procedures [16]. In brief, tumors were extracted, sectioned and fixed with cold acetone for 30 min. After blocking with 10% donkey serum for 60 min at RT, tissue slides were incubated with a primary mouse anti-human anti-CD38 antibody (1:400, Novus Biologicals) and rat anti-mouse anti-CD31 (1:100, ThermoFisher Scientific) overnight at 4 °C. The sections were then washed and stained with a secondary goat anti-mouse AlexaFluor488 and Cy3-labeled donkey anti-rat antibodies (ThermoFisher Scientific). Finally, slides were treated with DAPI-containing hard mounting medium (Vector Laboratories, USA) and imaged using a Nikon A1RS confocal microscope.

Statistical analysis

All data are denoted as Mean ± Standard Deviation. Testing for statistical significance was performed using a Student t-test. *P*-values less than 0.05 were considered statistically significant.

Results

CD38 expression screening in B-cell lymphoma cell lines

Relative expression levels of CD38 in five B-cell lymphoma cell lines (Ramos, Daudi, Raji, Rec-1, and HBL-1) were determined by Western blot. The 45-kDa green bands represented CD38, and 55-kDa red bands represented β-tubulin. Ramos cells showed the highest expression of CD38 while HBL-1 cells displayed the lowest CD38 expression, relative to the expression of β-tubulin (Fig. 1a).

Cellular binding affinity of daratumumab, Df-daratumumab, and ^{89}Zr-Df-daratumumab

Ramos and HBL-1 were analyzed by flow cytometry using daratumumab or Df-daratumumab as the primary antibody. Daratumumab and Df-daratumumab displayed similarly high levels of binding affinity in Ramos cells and comparably low levels in HBL-1

cells (Fig. 1b), suggesting Df conjugation does not affect the binding ability of daratumumab at high or low concentrations. ^{89}Zr-Df-daratumumab showed a radiolabeling yield of 89.80 ± 2.21% and specific activity of 71.0 ± 12.6 KBq/μg (n=11). The B_{max} and K_a of ^{89}Zr-Df-daratumumab in Ramos cells were quantified using a cellular affinity assay. The specific binding curve revealed that ^{89}Zr-Df-daratumumab reached its maximum binding at the concentration of approximately 3 nM, and had a K_a value of 1.29 ± 0.39 nM and a receptor density of (1.43 ± 0.16) $\times 10^5$ per cell for Ramos cells (Fig. 1c). These results demonstrated that ^{89}Zr-Df-daratumumab has a high binding affinity with Ramos cells.

PET imaging in lymphoma models

PET imaging was performed at 6, 12, 24, 48, 72, 96, and 120 h post-injection (p.i.) of ^{89}Zr-Df-daratumumab in Ramos and HBL-1 lymphoma models (Fig. 2). In maximum intensity projection (MIP) images, Ramos tumors exhibited high uptake while HBL-1 tumors displayed low tumor uptake at all time points post-injection. As a non-specific control probe, ^{89}Zr-Df-IgG could not delineate tumor sites at any time point. For both tumor models, ^{89}Zr radiolabeled daratumumab and IgG showed high uptake in the blood and blood-rich organs at early stages.

Quantitative data were obtained via ROI analyse of the tumor, heart (blood), liver and kidney at different time points (Fig. 3). After injection of ^{89}Zr-Df-daratumumab, Ramos tumors showed higher tracer uptake than HBL-1 tumor at all time points. PET imaging of ^{89}Zr-Df-daratumumab showed a substantial increase in tumor uptake from 9.6 ± 5.2 to 26.6 ± 8.0 %ID/g for Ramos models (n=4) whereas there was only an increase from 2.4 ± 0.8 to 6.6 ± 2.9 %ID/g for HBL-1 models (n = 4). ^{89}Zr radiolabeled non-specific IgG also demonstrated low tumor uptake increase from 2.2 ± 0.8 to 4.3 ± 0.8 %ID/g for Ramos. The uptake in other organs decreased after injection of ^{89}Zr-Df-daratumumab and ^{89}Zr-Df-IgG, with no significant differences. The difference in tumor uptake of both tracers suggested there was a specific accumulation of ^{89}Zr-Df-daratumumab for CD38-positive lymphoma.

Biodistribution

Ex vivo biodistribution studies were performed to verify the PET analysis (Fig. 4). After injection of ^{89}Zr-Df-daratumumab, Ramos tumors were found to have a substantially higher uptake at 23.2 ± 9.3 %ID/g than HBL-1 tumors at 3.7 ± 1.5 %ID/g after 120 h ($P < 0.05$, n=4). The tumor uptake of ^{89}Zr-Df-IgG in Ramos tumors was only 3.5 ± 0.6 %ID/g, which is also significantly lower than that of ^{89}Zr-Df-daratumumab, suggesting the non-specific tumor binding of Ramos tumors. In other organs, including the heart, liver, spleen, lung, and kidneys, ^{89}Zr-Df-daratumumab showed lower uptake in HBL-1 than the Ramos lymphoma model, which may be attributed to low level of tumor uptake and increased off-target accumulation. Given the bone-seeking nature of unbound ^{89}Zr *in vivo* and the fact that trans-chelated ^{89}Zr bound to plasma proteins normally displays a strong affinity for phosphate [17], bone uptake of tracers was found similar to previous studies, with uptake values of 7.21 ± 4.22, 8.45 ± 2.59, and 6.35 ± 0.45 %ID/g in Ramos, HBL-1, and non-specific IgG groups, respectively [15, 16].

Immunofluorescent staining of CD38 in lymphoma tumors

Immunofluorescent staining of tumor tissues verified the differential CD38 expression in different lymphoma models. Ramos tumor tissues showed higher expression of CD38 than HBL-1 tumor (Fig. 5). HBL-1 tumor tissues showed the near-background levels of CD38 staining. Anti-mouse CD31 staining displayed vessels in the tumor tissues. The CD38 staining intensity correlated well with the tumor uptakes shown in PET imaging analysis, further revealing the ability of ^{89}Zr-Df-daratumumab to visualize CD38 expression noninvasively in lymphoma.

Discussion

The biological hallmarks of cancer provided a promising era of cancer diagnosis and therapy through the development of targeted molecular therapies. Among them, targeted immunotherapy using mAbs has been considered a successful treatment for many forms of cancer [11, 18]. MAbs are capable of binding cancer cells specifically and kill the disseminated tumor while decreasing side-effects on normal tissues [19]. It is well known that some mAbs provide useful immunotherapy for the effective treatment of B-cell lymphomas. The anti-CD20 rituximab demonstrated a powerful therapeutic effect in B-cell lymphoma. However, B cells lose CD20 expression once they terminally differentiate into plasma cells [20]. Meanwhile, CD38 is highly and uniformly expressed on plasma cells and considered a biomarker for MM. In this study, we applied immunoPET for imaging of human CD38 in B-cell lymphoma xenograft models and further evaluate its targeting effect *in vivo*.

MM is a disease characterized by a monoclonal plasma cell population in bone marrow. To date, X-ray is the preliminary choice for detecting skeleton abnormality but has limited applications for small lesion and disease monitoring [21]. Low-dose whole-body computed tomography (WB-CT) and MRI have been proven useful for detection of myeloma [22]. However, these radiological methods could not represent the changes of MM cells, microenvironment or molecular targets. ^{18}F-FDG PET/CT has limitations including a lack of sensitivity for detecting diffuse bone marrow involvement, low-density plasmocyte infiltration, as well as some small skull lesions [23]. Other PET tracers have been developed that might be useful in the workup of patients with newly diagnosed and relapsing MM, including ^{11}C-MET for protein synthesis, 3’-deoxy-3’-^{18}F-fluorothymidine (^{18}F-FLT) for DNA synthesis, ^{11}C-acetate for amino acids synthesis, and so forth [24]. Although CD38 is considered a standard biomarker for immunophenotypic identification of MM [6, 11], clinical CD38 detection in bone marrow or extramedullary lesions can only be done using immunophenotypic or PCR-based molecular techniques [25]. Both techniques are invasive and occasionally yield false negative results for minor lesions. Our study showed the ability of ^{89}Zr-Df-daratumumab to visualize the specific expression of CD38 in B-cell lymphoma murine models. This immunoPET imaging probe may potentially provide a noninvasive method for detecting MM disease and evaluating the response to treatment in the clinic.

Although evaluating CD38 using imaging methods is of significant interest for the clinic, few studies were reported previously. For some MM clinical studies, CD38 levels were correlated with quantitative data such as SUV (sum of uptake value) of ^{18}F-FDG [26] or

^{99m}Tc-methoxyisobutylisonitrile [27], but the level of CD38 expression is still determined by invasive biopsy analysis. Radiolabeled daratumumab provides a method for visualizing CD38 levels *in vivo*. Moreover, preclinical data has shown encouraging results for daratumumab that it is well-tolerated and safe for imaging applications [15, 21]. To date, the only study for imaging of *in vivo* expression of CD38 was done recently by our group using ^{89}Zr labeled daratumumab in lung cancer murine models [14]. However, the relatively low tumor uptake of this radiolabeled antibody did not provide substantial evidence for practical application of CD38 imaging. This study is an extension of our previous study to evaluate the role of ^{89}Zr-Df-daratumumab in B-cell lymphoma. High tumor load of mAb demonstrated lower plasma concentration than expected [35]. Similarly, in our study, after the administration of ^{89}Zr-Df-daratumumab, blood uptake in the Ramos model was significantly lower than that in the HBL model. In previous studies, Burkitt's lymphoma Ramos and Daudi cells had CD38 receptors at the concentration of 200,000 to 300,000 molecules/cell, which was higher than the UM9 and L363 MM cell lines with less CD38 receptors at the concentration of 50,000 to 150,000 molecules/cell [12, 21]. Thus, ^{89}Zr-Df-daratumumab could be used in these B-cell lymphomas models, which is more clinically relevant.

Besides MM and some B-cell lymphomas, increased CD38 expression can also be found in some other diseases related with T-cell expression of CD38, including rheumatoid arthritis synovial tissues [28], systemic lupus erythematosus [29], HIV infection [30] [31], and liver transplantation rejection [32]. Due to its ability to image CD38 *in vivo*, ^{89}Zr-Df-daratumumab may be preclinically applied for evaluating CD38 expression which correlated with disease diagnosis assistance and progression. ^{89}Zr-Df-daratumumab may also provide a method to monitor CD38 expression after CD38-targeted treatment. Additionally, CD38 expression on T cells plays an important role in many immune-related diseases [28, 29, 32]. CD38 has also been considered a novel immune checkpoint protein which is incorporated in the PD-1 blockade to prevent immune resistance [33]. Therefore, immunoPET imaging using ^{89}Zr-Df-daratumumab could provide insight into personal evaluation of CD38 expression noninvasively in various CD38 related diseases [34].

Due to the long circulation half-life of full antibodies, the imaging of these antibodies requires a radionuclide with a relatively long half-life, such as ^{89}Zr. However, antibodies directly labeled with ^{89}Zr may present unwanted clinical complications: long delays between the injection of radiotracer and optimal imaging times as well as unnecessarily high radiation dose rates to healthy tissues [34]. For improved clinical application, an optimized choice to reduce extended circulation is to utilize an antibody fragment with a smaller size [36–38]. ^{64}Cu radiolabeled F(ab')$_2$ fragment was predicted to have a 3.3-fold reduction of total body dose in humans with 0.015 mSv/MBq, compared to the labeled full antibody [37]. However, antibody fragments might have decreased affinity. Another potential approach is the pre-targeting PET imaging strategy via "click chemistry". For example, the specificity and affinity of trans-cyclooctene (TCO) and tetrazine (Tz) system can make a readily accessible pre-targeting imaging sytem, which may lead to a higher than 25-fold decrease in absorbed dose for the total body and at least a 15-fold decrease in each tissue [39]. Other targeted radiolabeled peptides or small molecules have displayed some advantages in the era of cancer imaging. In comparison with ImmunoPET imaging agents derived from

commercial or FDA approved antibodies, most small molecules are usually not commercially available which makes it difficult to be spread in the clinic. Combinatorial methods including chemical biology, synthetic small molecule compounds and nanomaterials might improve pharmacological behavior [3].

The excellent results obtained from the daratumumab treatment in patients with relapsed/refractory MM intensified the interest in the area of radiation treatment combined with immunotherapy targeting CD38. A few radiolabeled anti-CD20 antibodies in lymphoma are successful examples [40]. For CD38 targeting, one study employed a pre-targeted system using an anti-CD38 antibody-streptavidin complex and ^{90}Y-DOTA-biotin for eradicating subcutaneous plasmocytoma xenografts [41]. Another study applied an α-emitter ^{213}Bi labeled anti-CD38 mAb intraperitoneally to treat MM cells and xenografts [42]. To evaluate the response of CD38 targeting treatment, PET imaging of ^{89}Zr-Df-daratumumab could provide a very direct method. Furthermore, a theranostic role of radiolabeled daratumumab might provide another potential clinical application in the future.

Conclusions

In conclusion, we investigated ^{89}Zr-Df-daratumumab for PET imaging to evaluate CD38 expression noninvasively in B-cell lymphoma. ^{89}Zr-Df-daratumumab displayed specific, rapid, and persistent accumulation in tumors with high CD38 expression. Our study indicates that radiolabeled daratumumab is a promising PET tracer for CD38-positive hematological diseases such as MM in future clinical applications.

Acknowledgments

This work was supported by the University of Wisconsin - Madison, the National Institutes of Health (NIBIB/NCI 1R01CA169365, 1R01EB021336, P30CA014520, T32CA009206), the American Cancer Society (125246-RSG-13-099-01-CCE), the National Natural Science Foundation of China (81441051, 81401465, 51573096), the Beijing Nova Program (Z171100001117024), the Beijing Capital Special Development Application Program (Z141107002514159), and the Basic Research Program of Shenzhen (JCYJ20170412111100742, JCYJ20160422091238319)

References

1. Swerdlow SH, Campo E, Pileri SA, Harris NL, Stein H, Siebert R, et al. The 2016 revision of the World Health Organization classification of lymphoid neoplasms. Blood. 2016; 127:2375–90. DOI: 10.1182/blood-2016-01-643569 [PubMed: 26980727]
2. Regelink JC, Minnema MC, Terpos E, Kamphuis MH, Raijmakers PG, Pieters-van den Bos IC, et al. Comparison of modern and conventional imaging techniques in establishing multiple myeloma-related bone disease: a systematic review. Br J Haematol. 2013; 162:50–61. DOI: 10.1111/bjh.12346 [PubMed: 23617231]
3. Ehlerding EB, England CG, McNeel DG, Cai W. Molecular Imaging of Immunotherapy Targets in Cancer. J Nucl Med. 2016; 57:1487–92. DOI: 10.2967/jnumed.116.177493 [PubMed: 27469363]
4. van Dongen GA, Visser GW, Lub-de Hooge MN, de Vries EG, Perk LR. Immuno-PET: a navigator in monoclonal antibody development and applications. Oncologist. 2007; 12:1379–89. DOI: 10.1634/theoncologist.12-12-1379 [PubMed: 18165614]
5. Malavasi F, Deaglio S, Funaro A, Ferrero E, Horenstein AL, Ortolan E, et al. Evolution and function of the ADP ribosyl cyclase/CD38 gene family in physiology and pathology. Physiol Rev. 2008; 88:841–86. DOI: 10.1152/physrev.00035.2007 [PubMed: 18626062]

6. Deaglio S, Mehta K, Malavasi F. Human CD38: a (r)evolutionary story of enzymes and receptors. Leuk Res. 2001; 25:1–12. [PubMed: 11137554]
7. Sanchez L, Wang Y, Siegel DS, Wang ML. Daratumumab: a first-in-class CD38 monoclonal antibody for the treatment of multiple myeloma. J Hematol Oncol. 2016; 9:51.doi: 10.1186/s13045-016-0283-0 [PubMed: 27363983]
8. Malavasi F, Deaglio S, Damle R, Cutrona G, Ferrarini M, Chiorazzi N. CD38 and chronic lymphocytic leukemia: a decade later. Blood. 2011; 118:3470–8. DOI: 10.1182/blood-2011-06-275610 [PubMed: 21765022]
9. Amaya-Chanaga CI, Rassenti LZ. Biomarkers in chronic lymphocytic leukemia: Clinical applications and prognostic markers. Best Pract Res Clin Haematol. 2016; 29:79–89. DOI: 10.1016/j.beha.2016.08.005 [PubMed: 27742074]
10. Lokhorst HM, Plesner T, Laubach JP, Nahi H, Gimsing P, Hansson M, et al. Targeting CD38 with Daratumumab Monotherapy in Multiple Myeloma. N Engl J Med. 2015; 373:1207–19. DOI: 10.1056/NEJMoa1506348 [PubMed: 26308596]
11. de Weers M, Tai YT, van der Veer MS, Bakker JM, Vink T, Jacobs DC, et al. Daratumumab, a novel therapeutic human CD38 monoclonal antibody, induces killing of multiple myeloma and other hematological tumors. J Immunol. 2011; 186:1840–8. DOI: 10.4049/jimmunol.1003032 [PubMed: 21187443]
12. Overdijk MB, Verploegen S, Bogels M, van Egmond M, Lammerts van Bueren JJ, Mutis T, et al. Antibody-mediated phagocytosis contributes to the anti-tumor activity of the therapeutic antibody daratumumab in lymphoma and multiple myeloma. MAbs. 2015; 7:311–21. DOI: 10.1080/19420862.2015.1007813 [PubMed: 25760767]
13. Overdijk MB, Jansen JH, Nederend M, Lammerts van Bueren JJ, Groen RW, Parren PW, et al. The Therapeutic CD38 Monoclonal Antibody Daratumumab Induces Programmed Cell Death via Fcgamma Receptor-Mediated Cross-Linking. J Immunol. 2016; 197:807–13. DOI: 10.4049/jimmunol.1501351 [PubMed: 27316683]
14. Ehlerding EB, England CG, Jiang D, Graves SA, Kang L, Lacognata S, et al. CD38 as a PET Imaging Target in Lung Cancer. Mol Pharm. 2017; 14:2400–6. DOI: 10.1021/acs.molpharmaceut.7b00298 [PubMed: 28573863]
15. Hong H, Severin GW, Yang Y, Engle JW, Zhang Y, Barnhart TE, et al. Positron emission tomography imaging of CD105 expression with 89Zr-Df-TRC105. Eur J Nucl Med Mol Imaging. 2012; 39:138–48. DOI: 10.1007/s00259-011-1930-x [PubMed: 21909753]
16. England CG, Ehlerding EB, Hernandez R, Rekoske BT, Graves SA, Sun H, et al. Preclinical Pharmacokinetics and Biodistribution Studies of 89Zr-Labeled Pembrolizumab. J Nucl Med. 2017; 58:162–8. DOI: 10.2967/jnumed.116.177857 [PubMed: 27493273]
17. Abou DS, Ku T, Smith-Jones PM. In vivo biodistribution and accumulation of 89Zr in mice. Nucl Med Biol. 2011; 38:675–81. DOI: 10.1016/j.nucmedbio.2010.12.011 [PubMed: 21718943]
18. Bailly C, Clery PF, Faivre-Chauvet A, Bourgeois M, Guerard F, Haddad F, et al. Immuno-PET for Clinical Theranostic Approaches. Int J Mol Sci. 2016; 18doi: 10.3390/ijms18010057
19. Wright BD, Lapi SE. Designing the magic bullet? The advancement of immuno-PET into clinical use. J Nucl Med. 2013; 54:1171–4. DOI: 10.2967/jnumed.113.126086 [PubMed: 23908265]
20. Zojer N, Kirchbacher K, Vesely M, Hubl W, Ludwig H. Rituximab treatment provides no clinical benefit in patients with pretreated advanced multiple myeloma. Leuk Lymphoma. 2006; 47:1103–9. DOI: 10.1080/10428190600564803 [PubMed: 16840202]
21. Dimopoulos M, Terpos E, Comenzo RL, Tosi P, Beksac M, Sezer O, et al. International myeloma working group consensus statement and guidelines regarding the current role of imaging techniques in the diagnosis and monitoring of multiple Myeloma. Leukemia. 2009; 23:1545–56. DOI: 10.1038/leu.2009.89 [PubMed: 19421229]
22. Dimopoulos MA, Hillengass J, Usmani S, Zamagni E, Lentzsch S, Davies FE, et al. Role of magnetic resonance imaging in the management of patients with multiple myeloma: a consensus statement. J Clin Oncol. 2015; 33:657–64. DOI: 10.1200/JCO.2014.57.9961 [PubMed: 25605835]
23. Bartel TB, Haessler J, Brown TL, Shaughnessy JD Jr, van Rhee F, Anaissie E, et al. F18-fluorodeoxyglucose positron emission tomography in the context of other imaging techniques and

prognostic factors in multiple myeloma. Blood. 2009; 114:2068–76. DOI: 10.1182/blood-2009-03-213280 [PubMed: 19443657]

24. de Waal EG, Glaudemans AW, Schroder CP, Vellenga E, Slart RH. Nuclear medicine imaging of multiple myeloma, particularly in the relapsed setting. Eur J Nucl Med Mol Imaging. 2017; 44:332–41. DOI: 10.1007/s00259-016-3576-1 [PubMed: 27900520]
25. Rajkumar SV, Harousseau JL, Durie B, Anderson KC, Dimopoulos M, Kyle R, et al. Consensus recommendations for the uniform reporting of clinical trials: report of the International Myeloma Workshop Consensus Panel 1. Blood. 2011; 117:4691–5. DOI: 10.1182/blood-2010-10-299487 [PubMed: 21292775]
26. Ak I, Gulbas Z. F-18 FDG uptake of bone marrow on PET/CT scan: it's correlation with CD38/CD138 expressing myeloma cells in bone marrow of patients with multiple myeloma. Ann Hematol. 2011; 90:81–7. DOI: 10.1007/s00277-010-1037-7 [PubMed: 20690019]
27. Ak I, Aslan V, Vardareli E, Gulbas Z. Tc-99m methoxyisobutylisonitrile bone marrow imaging for predicting the levels of myeloma cells in bone marrow in multiple myeloma: correlation with CD38/CD138 expressing myeloma cells. Ann Hematol. 2003; 82:88–92. DOI: 10.1007/s00277-002-0600-2 [PubMed: 12601486]
28. Chang X, Yue L, Liu W, Wang Y, Wang L, Xu B, et al. CD38 and E2F transcription factor 2 have uniquely increased expression in rheumatoid arthritis synovial tissues. Clin Exp Immunol. 2014; 176:222–31. DOI: 10.1111/cei.12268 [PubMed: 24397353]
29. Pavon EJ, Zumaquero E, Rosal-Vela A, Khoo KM, Cerezo-Wallis D, Garcia-Rodriguez S, et al. Increased CD38 expression in T cells and circulating anti-CD38 IgG autoantibodies differentially correlate with distinct cytokine profiles and disease activity in systemic lupus erythematosus patients. Cytokine. 2013; 62:232–43. DOI: 10.1016/j.cyto.2013.02.023 [PubMed: 23538292]
30. Lins L, Farias E, Brites-Alves C, Torres A, Netto EM, Brites C. Increased expression of CD38 and HLADR in HIV-infected patients with oral lesion. J Med Virol. 2017; 89:1782–7. DOI: 10.1002/jmv.24852 [PubMed: 28500735]
31. Dentone C, Fenoglio D, Schenone E, Cenderello G, Prinapori R, Signori A, et al. Increased CD38 expression on T lymphocytes as a marker of HIV dissemination into the central nervous system. HIV Clin Trials. 2015; 16:190–6. DOI: 10.1179/1945577115Y.0000000005 [PubMed: 26365593]
32. Boix F, Millan O, San Segundo D, Mancebo E, Rimola A, Fabrega E, et al. High expression of CD38, CD69, CD95 and CD154 biomarkers in cultured peripheral T lymphocytes correlates with an increased risk of acute rejection in liver allograft recipients. Immunobiology. 2016; 221:595–603. DOI: 10.1016/j.imbio.2016.01.008 [PubMed: 26850323]
33. Shallis RM, Terry CM, Lim SH. The multi-faceted potential of CD38 antibody targeting in multiple myeloma. Cancer Immunol Immunother. 2017; 66:697–703. DOI: 10.1007/s00262-017-1990-2 [PubMed: 28341874]
34. Kraeber-Bodere F, Bailly C, Cherel M, Chatal JF. ImmunoPET to help stratify patients for targeted therapies and to improve drug development. Eur J Nucl Med Mol Imaging. 2016; 43:2166–8. DOI: 10.1007/s00259-016-3458-6 [PubMed: 27539021]
35. Funaro A, Horenstein AL, Calosso L, Morra M, Tarocco RP, Franco L, et al. Identification and characterization of an active soluble form of human CD38 in normal and pathological fluids. Int Immunol. 1996; 8:1643–50. [PubMed: 8943558]
36. Luo H, Hernandez R, Hong H, Graves SA, Yang Y, England CG, et al. Noninvasive brain cancer imaging with a bispecific antibody fragment, generated via click chemistry. Proc Natl Acad Sci U S A. 2015; 112:12806–11. DOI: 10.1073/pnas.1509667112 [PubMed: 26417085]
37. Lam K, Chan C, Reilly RM. Development and preclinical studies of 64Cu-NOTA-pertuzumab F(ab')2 for imaging changes in tumor HER2 expression associated with response to trastuzumab by PET/CT. MAbs. 2017; 9:154–64. DOI: 10.1080/19420862.2016.1255389 [PubMed: 27813707]
38. Zhang Y, Hong H, Orbay H, Valdovinos HF, Nayak TR, Theuer CP, et al. PET imaging of CD105/endoglin expression with a (6)(1)/(6)(4)Cu-labeled Fab antibody fragment. Eur J Nucl Med Mol Imaging. 2013; 40:759–67. DOI: 10.1007/s00259-012-2334-2 [PubMed: 23344138]
39. Houghton JL, Zeglis BM, Abdel-Atti D, Sawada R, Scholz WW, Lewis JS. Pretargeted Immuno-PET of Pancreatic Cancer: Overcoming Circulating Antigen and Internalized Antibody to Reduce

Radiation Doses. J Nucl Med. 2016; 57:453–9. DOI: 10.2967/jnumed.115.163824 [PubMed: 26471693]

40. Witzig TE, Gordon LI, Cabanillas F, Czuczman MS, Emmanouilides C, Joyce R, et al. Randomized controlled trial of yttrium-90-labeled ibritumomab tiuxetan radioimmunotherapy versus rituximab immunotherapy for patients with relapsed or refractory low-grade, follicular, or transformed B-cell non-Hodgkin's lymphoma. J Clin Oncol. 2002; 20:2453–63. DOI: 10.1200/JCO.2002.11.076 [PubMed: 12011122]
41. Green DJ, Orgun NN, Jones JC, Hylarides MD, Pagel JM, Hamlin DK, et al. A preclinical model of CD38-pretargeted radioimmunotherapy for plasma cell malignancies. Cancer Res. 2014; 74:1179–89. DOI: 10.1158/0008-5472.CAN-13-1589 [PubMed: 24371230]
42. Teiluf K, Seidl C, Blechert B, Gaertner FC, Gilbertz KP, Fernandez V, et al. alpha-Radioimmunotherapy with (2)(1)(3)Bi-anti-CD38 immunoconjugates is effective in a mouse model of human multiple myeloma. Oncotarget. 2015; 6:4692–703. DOI: 10.18632/oncotarget.2986 [PubMed: 25576914]

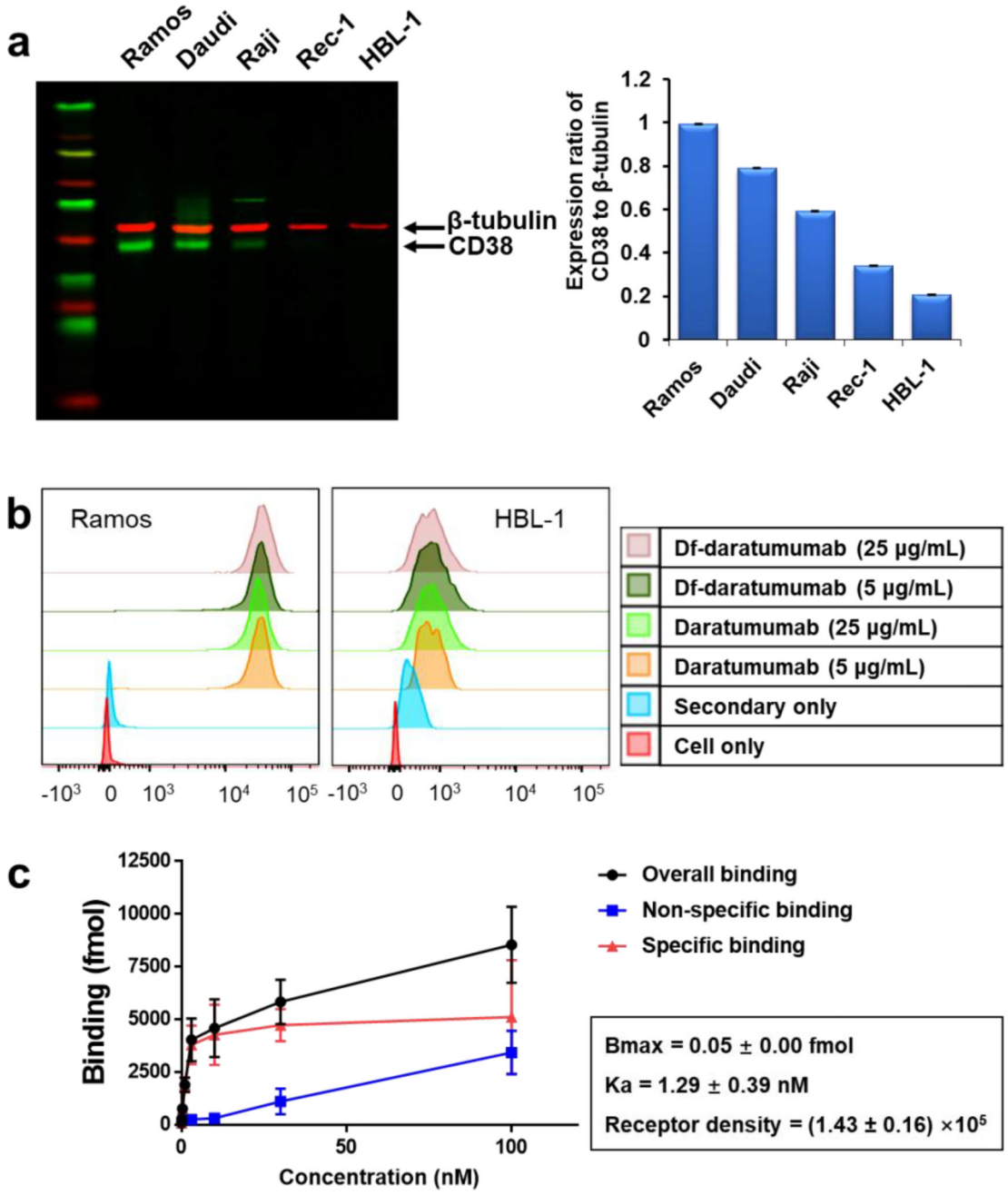

Figure 1.

In vitro analysis of CD38 expression and binding ability of daratumumab to lymphoma cells. (**a**) Western blot analysis showed CD38 expression was highest for Ramos cells and lowest expression for HBL-1 cells among five B-cell lymphoma cell lines. (**b**) Flow cytometry verified the differential expression of CD38 in Ramos and HBL-1 cell lines and displayed similar binding ability of Df-conjugated daratumumab. (**c**) Cellular binding assay showed ^{89}Zr-Df-daratumumab bound specifically to Ramos cells, with a K_a value of 1.29 ± 0.39 nM.

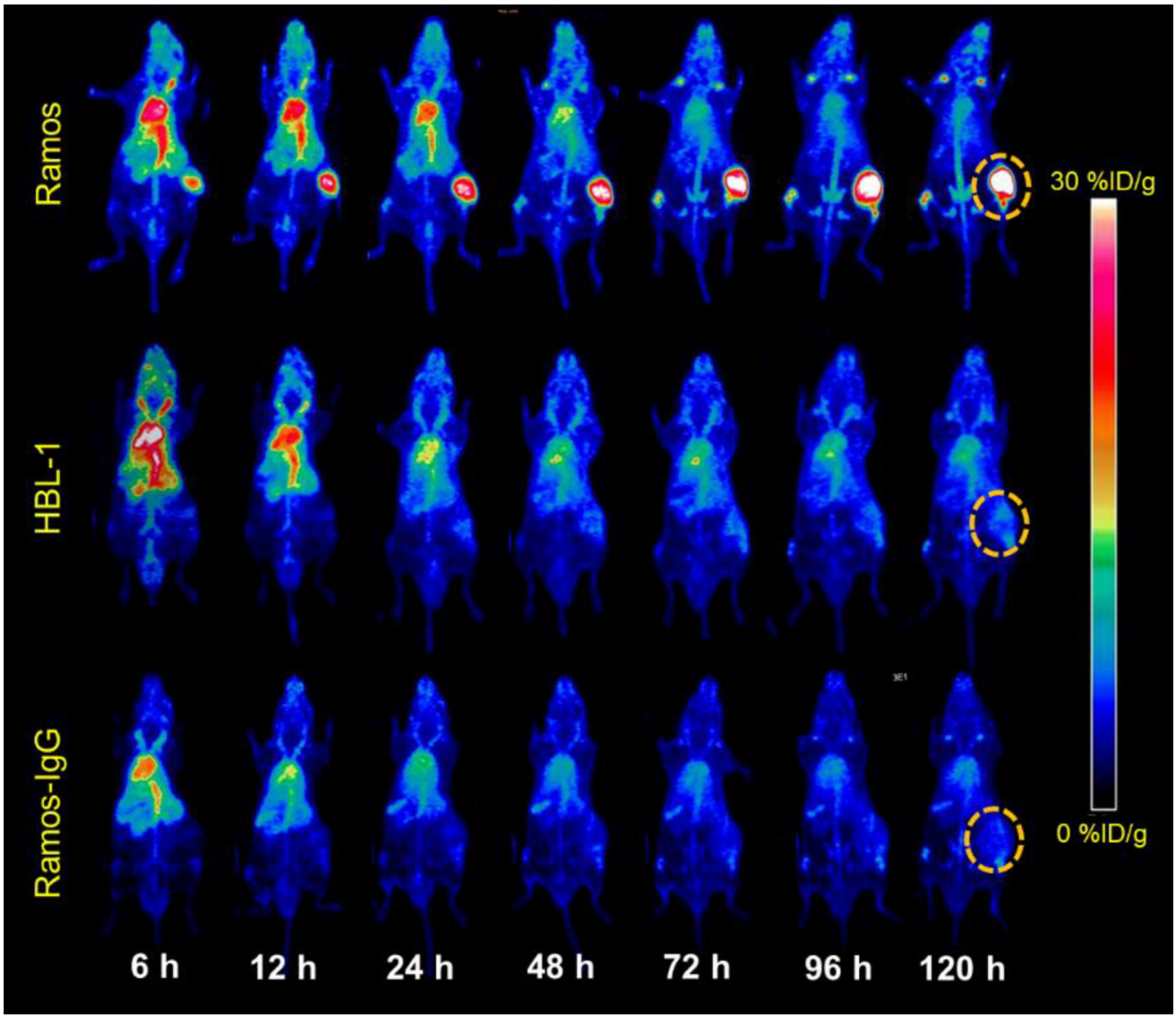

Figure 2.

PET maximum intensity projection (MIP) images of Ramos and HBL-1 lymphoma tumor bearing models from 6 to 120 h post-injection. Following injection of ^{89}Zr-Df-daratumumab, Ramos tumors displayed higher uptake than HBL-1 tumors at all time points. After injection of a ^{89}Zr-Df-IgG, Ramos tumors demonstrated significantly decreased uptake at the same time points. Tumors are indicated by dashed circles.

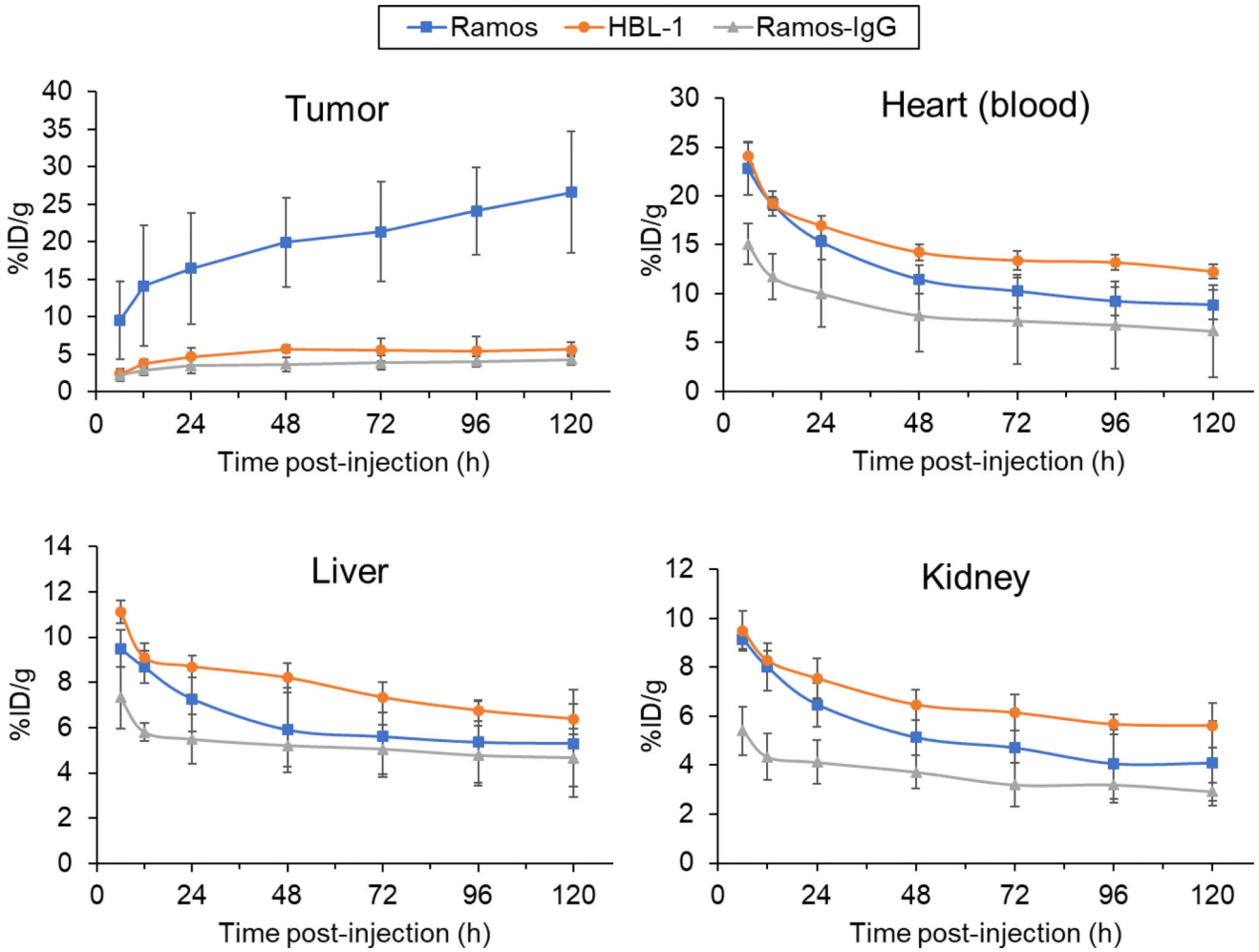

Figure 3.

Quantitative results of PET imaging after injection of ^{89}Zr-Df-daratumumab or ^{89}Zr-Df-IgG in Ramos and HBL-1 lymphoma models. At all of the time points, Ramos tumors displayed significantly higher uptake than HBL-1 tumors and the nonspecific tracer ($p < 0.05$; $n = 4$). The uptake of ^{89}Zr-Df-daratumumab in the heart blood pool, liver, and kidney showed no significant difference between Ramos and HBL-1 models.

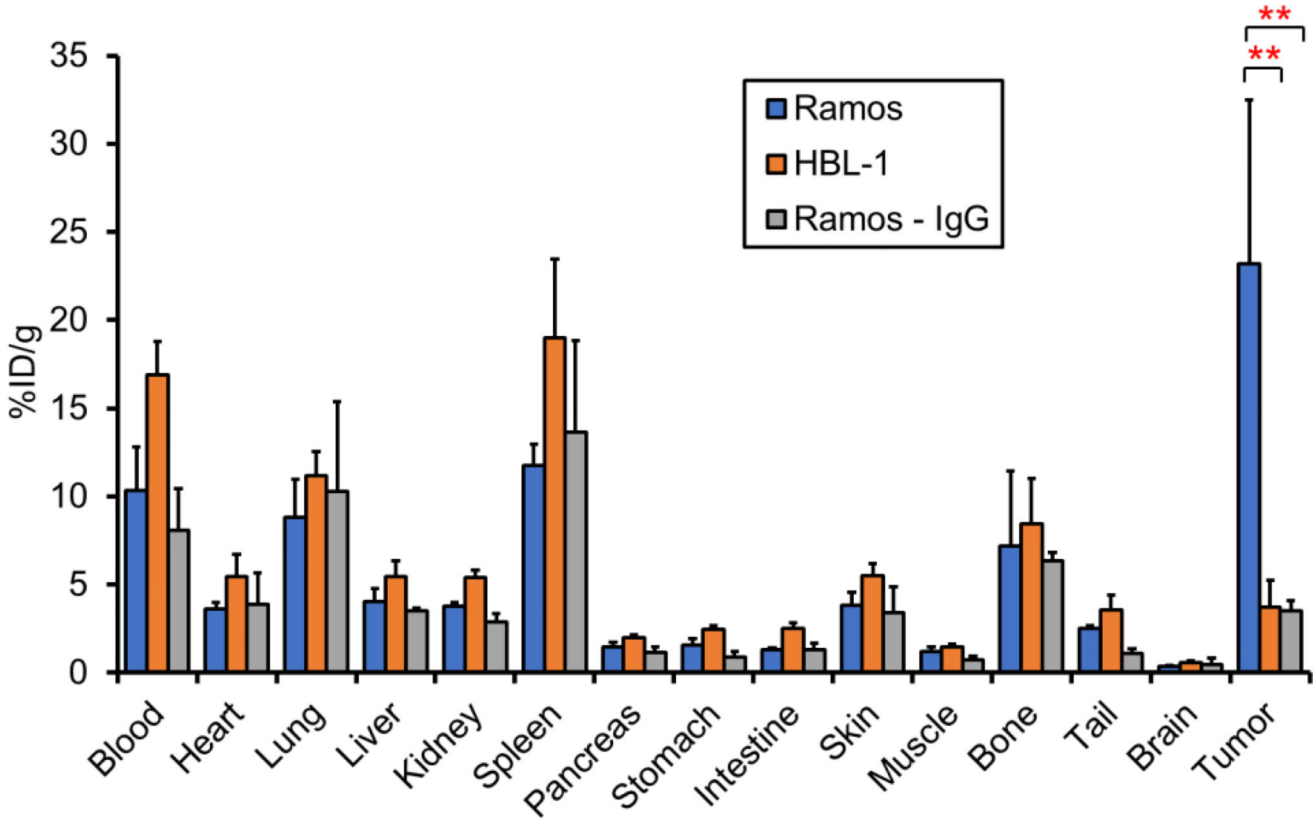

Figure 4.

Biodistribution results at 120 h p.i. of ^{89}Zr-Df-daratumumab or ^{89}Zr-Df-IgG. Ramos tumors showed significantly higher uptake than HBL-1 tumors and nonspecific IgG group, which verified the results from PET imaging. Both radiolabeled daratumumab and IgG showed relatively high uptake in blood and blood-rich organs, such as lungs, spleen. **$p < 0.01$; $n = 4$.

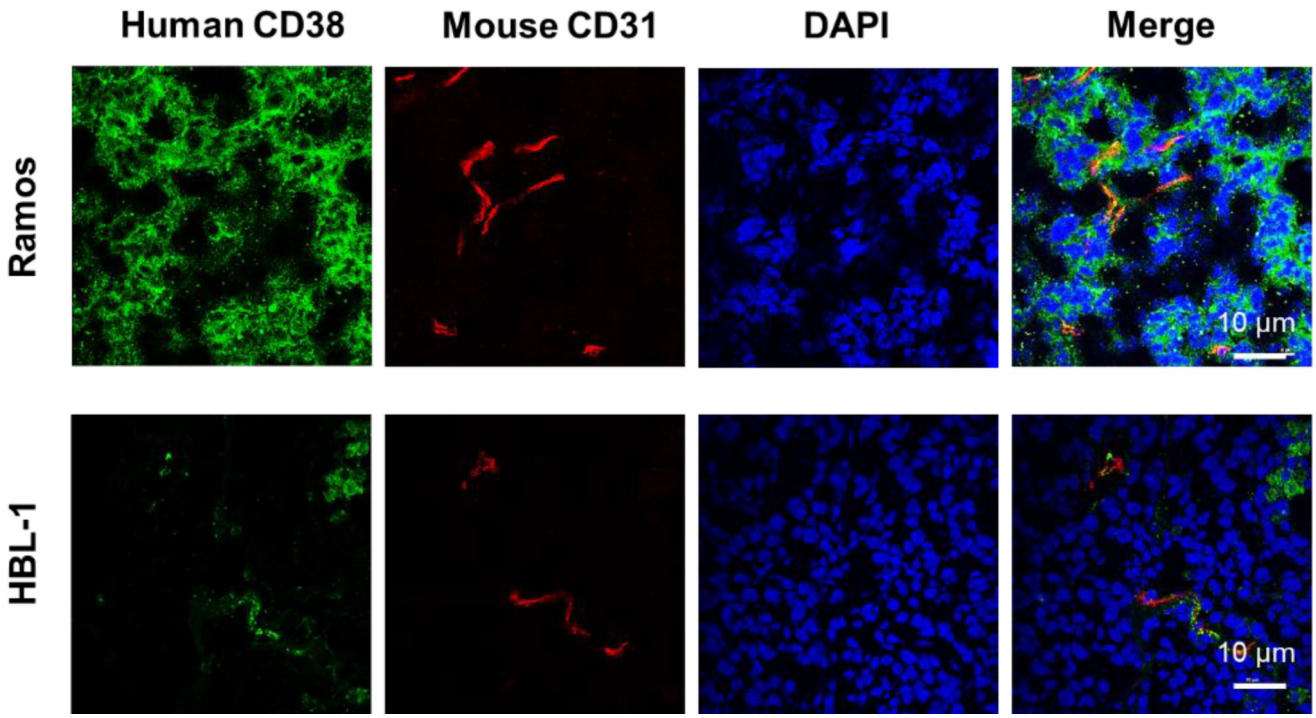

Figure 5.

Immunofluorescence staining of tumor tissue sections. Ramos tumors displayed a higher level of green staining signals on the cell surface, verifying higher CD38 expression in Ramos tumors. Scale bar: 10 μm.